

Perspectives for a mixed two-qubit system with binomial quantum states

Mahmoud Abdel-Aty§

Mathematics Department, Faculty of Science, South Valley University, 82524 Sohag, Egypt.

Abstract.

The problem of the relationship between entanglement and two-qubit systems in which it is embedded is central to the quantum information theory. This paper suggests that the concurrence hierarchy as an entanglement measure provides an alternative view of how to think about this problem. We consider mixed states of two qubits and obtain an exact solution of the time-dependent master equation that describes the evolution of two two-level qubits (or atoms) within a perfect cavity for the case of multiphoton transition. We consider the situation for which the field may start from a binomial state. Employing this solution, the significant features of the entanglement when a second qubit is weakly coupled to the field and becomes entangled with the first qubit, is investigated. We also describe the response of the atomic system as it varies between the Rabi oscillations and the collapse-revival mode and investigate the atomic inversion and the Q-function. We identify and numerically demonstrate the region of parameters where significantly large entanglement can be obtained. Most interestingly, it is shown that features of the entanglement is influenced significantly when the multi-photon process is involved. Finally, we obtain illustrative examples of some novel aspects of this system and show how the off-resonant case can sensitize entanglement to the role of initial state setting.

PACS numbers: 32.80.-t, 42.50.Ct, 03.65.Ud, 03.65.Yz

Submitted to: *J. Opt. B: Quantum Semiclass. Opt.*

1. Overview

As a lot of researchers suggest [1-5], entanglement is one of the most mysterious aspects of quantum physics. Although it is by now possible to verify the predictions of entanglement theory in a variety of experiments [2], there remains a considerable gap between the formal definition of entanglement and the observable effects that are associated with this property. A major thrust of current research is to find a quantitative measure of entanglement for general states. For the experiments in the newest fields of physics, quantum computing, quantum communication, and quantum cryptography [6-13] the quantitative analysis of the multi-qubit or ion is of substantial interest [14]. The dipole-dipole interaction between two atoms can be understood through the exchange of virtual photons and depends on the transition dipole moment of the levels involved. It can be characterized by complex coupling constants, or by their real and imaginary parts, where the former affect decay constants and the latter lead to level shifts [15,16]. There is an inherent interest in analytical and non-perturbative solutions of multi-atom interacting with the cavity field problems, all the more considering quantum systems with more than one qubit. One examples of such kind is the system of two two-level qubits in an electromagnetic field [14-26]. Entanglement of identical qubits is a property dependent on which single-qubit basis is chosen, as any operation should act on each identical qubit in the same way. Indeed, individual qubits are excitations of a quantum field, and the single-qubit basis defines which set of qubits are used in representing the many-qubit state [27]. The analysis of entanglement sharing of the two-atom Tavis-Cummings model has been discussed in Ref. [28]. Recently, interest has mounted in exploring the quantum system composed of two qubits interacting with a thermal field [29]. We have addressed a general two-qubit system in a recent paper [23] in which an analytical expression for the temporal evolution of the Pancharatnam phase when the field starts from vacuum state is given.

This has motivated us to criticize the conception of entanglement of a two-qubit system in the context of the mixed quantum states. The main contribution of this paper is to synthesize conceptual insights that already exist to push forward a more coherent view of how concurrence as an entanglement measure of a two-qubit system might make progress in understanding the two-qubit entanglement. To be more precise, we assume that two two-level atoms (two qubits) share a bipartite system, taking into account the multi-photon transition. Another principal aim is to elucidate the extent to which mixed entangled states can affect the entanglement. The emphasis being put on the investigation of the entanglement in a more general situation in which the two atoms (qubits) share a mixed state, rather than a pure state and we propose to use the concurrence hierarchy as a measurement of entanglement [30-32]. The issue of attributing objective properties to the constituents of a quantum system composed of two qubits, does not turn out to be a straightforward generalization of the just analyzed case involving distinguishable qubits, and the problem of entanglement has to be reconsidered. Entangled mixed states may arise when one or both qubits of an

initially pure entangled state interact, intentionally or inadvertently, with other quantum degrees of freedom resulting in a non-unitary evolution of the pure state into a mixed state. In general it is known that there are also cases when entangled states are mixed with other entangled states and where the sum is separable.

The rest of the paper is organized as follows. We devote section 2 to give a brief overview of the binomial states and initial states setting. In section 3, we present notations and definitions of the model and its analytical solution to be used in the rest of the paper. Section 4 is devoted to consider the atomic inversion as well as the quasiprobability distribution. The concurrence as an entanglement measure is presented in section 5, followed by a numerical computation in which we shall examine the influence of different involved parameters in subsection 5.1. The paper is closes with the conclusions outlined in section 6.

2. Binomial state

The implementation independence in quantum information theory is guaranteed by the use of Hilbert spaces, states and operations between and on them. It is not said, what they physically describe in more concrete terms, whether we are dealing with spins, polarizations, energy levels, qubit numbers, or whatever you can imagine. The features of nonclassical states visualize specific aspects of nonclassicality and do not yield a complete characterization of nonclassicality as a phenomenon on its own. In this section we give a brief overview of the binomial states [33]. For measuring the quantum state of the radiation field, balanced homodyning has become a well established method, it directly measures phase sensitive quadrature distributions. Alternatively, unbalanced homodyning yields access to phase-space functions. For some systems, such as a cavity-field mode and a mode of the quantized motion of a trapped ion, methods have been proposed that allow for a direct detection of the characteristic functions of the quadratures. The binomial states are finite linear combinations of number states [33]

$$|\eta, m\rangle = \sum_{n=0}^{\infty} \left[\binom{m}{n} \eta^n (1-\eta)^{m-n} \right]^{1/2} |n\rangle, \quad (1)$$

which interpolate between some fundamental states such as number states and coherent states, where m is a non-negative integer, η is areal probability ($0 < \eta < 1$) and $|n\rangle$ is a number state of the radiation field. Such states have been studied in great detail in the literature (see e.g. Ref. [34]). The binomial states have the properties

$$|\eta, m\rangle = \begin{cases} |m\rangle & \eta \rightarrow 1 \\ |0\rangle & \eta \rightarrow 0 \\ |\alpha\rangle & \eta \rightarrow 0, \quad m \rightarrow \infty, \quad \eta m = \alpha^2. \end{cases} \quad (2)$$

In the theory of open system or the reduction theory, one often considers two subsystem A and F represented by Hilbert space. Let \mathfrak{S}_j , ($j = A, F$) be state spaces (the set of

all density operators) and $\mathfrak{S}_A \otimes \mathfrak{S}_F$ denotes the state space in the composite system. Here, we assume that, before entering the cavity, the field initially in a binomial state such as

$$\varpi = |\eta, m\rangle\langle\eta, m| \in \mathfrak{S}_F. \quad (3)$$

In pure-state quantum mechanics the state of the system is usually represented by a normalized wavefunction, which is a unit vector in a Hilbert space. Entangled mixed states may arise when the qubits of an initially pure entangled state interact, intentionally or inadvertently, with other quantum degrees of freedom resulting in a non-unitary evolution of the pure state into a mixed state. In general it is known that there are also cases when entangled states are mixed with other entangled states and where the sum is separable. The usual interpretation of mixed states, is that their creation involves irreversibly destroying information [35,36]. This has interesting consequences concerning entanglement theory, since there, the irreversibility is often associated with the fact that one is dealing with mixed states. We assume that, the two two-level qubits initially prepared in the mixed states enter the cavity whose single mode under consideration, prior to the interaction with the qubits, is in the binomial state ϖ . Thus, the atomic density matrix is of the diagonal form

$$\rho_i^{a_i}(0) = \cos^2 \theta_i |e_i\rangle\langle e_i| + \sin^2 \theta_i |g_i\rangle\langle g_i| \in \mathfrak{S}_{A_i}, \quad (4)$$

where $\rho_i^{a_i}(0)$ is the atomic density matrix for the i^{th} qubit. The initial state of the two qubits system can be written as

$$\rho^a(0) = \rho_1^a(0) \otimes \rho_2^a(0) \in \mathfrak{S}_A. \quad (5)$$

It is well known that mixed states can be realized by an ensemble of pure states in an infinite number of ways. The determination of the separability of a state and the determination of its entanglement have in common that a particular realization of a state has to be found such that some property holds for all pure states in that realization. In order to find this optimal realization, it is of considerable interest to have a mathematically elegant way of generating all possible realizations of a state [31].

3. Model for pair of qubits

We consider a mechanism through which a system of two qubits can be entangled in a cavity field. We assume that the qubits are modeled by two-level systems having multiphoton transition, which is a micromaser system [21]. The micromaser is an experimental realization of the idealized system of a two-level qubit interacting with a second quantized single-mode of the electromagnetic field [22]. In this section we consider a theoretical model which differs from the standard micromaser set-up in that instead of a single qubit we have assumed a pair of qubits interacting with a single mode of the cavity field (see figure 1). In the dipole and rotating wave approximation, one can write ($\hbar = 1$)

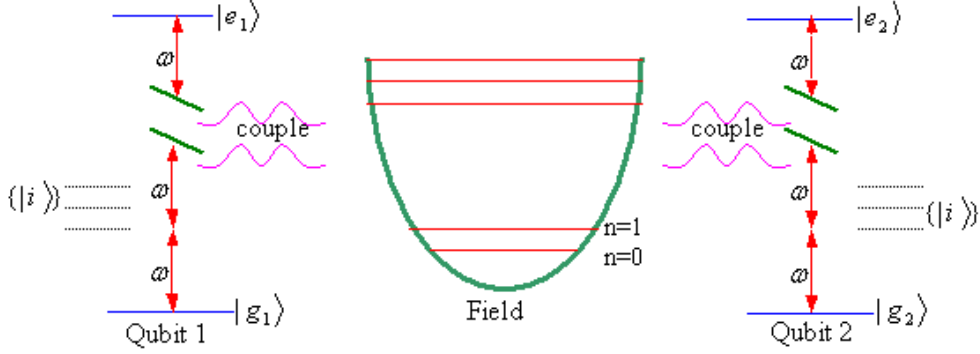


Figure 1. Schematic of the multiphoton transition in the interaction of a pair of two-level qubits with a single-mode radiation field. In the shown process we denote by $|e_j\rangle(|g_j\rangle)$ the j^{th} qubit's upper (lower) level and $\{|i\rangle\}$ are the virtual levels.

$$\begin{aligned} \hat{H} = & \omega \hat{a}^\dagger \hat{a} + \omega_1 [S_{ee}^{(1)} - S_{gg}^{(1)}] + \omega_2 [S_{ee}^{(2)} - S_{gg}^{(2)}] + \hat{a}^\dagger \hat{a} \{ \beta_1^{(1)} \hat{\sigma}_-^{(1)} \hat{\sigma}_+^{(1)} \\ & + \beta_1^{(2)} \hat{\sigma}_-^{(2)} \hat{\sigma}_+^{(2)} + \beta_2^{(1)} \hat{\sigma}_+^{(1)} \hat{\sigma}_-^{(1)} + \beta_2^{(2)} \hat{\sigma}_+^{(2)} \hat{\sigma}_-^{(2)} \} \Theta(k) + \gamma_1 S_{eg}^{(1)} \hat{a}^k \\ & + \gamma_1^* S_{ge}^{(1)} \hat{a}^{\dagger k} + \gamma_2 S_{eg}^{(2)} \hat{a}^k + \gamma_2^* \hat{a}^{\dagger k} S_{ge}^{(2)}. \end{aligned} \quad (6)$$

We denote by $S_{lm}^{(i)}$ the atomic operators for the i^{th} qubit. \hat{a} and \hat{a}^\dagger are field operators corresponding to annihilation and creation of photons in the cavity mode. We denote by γ_i the coupling constant for the i^{th} qubit, ω is the field frequency and ω_i is the atomic frequency for the i^{th} qubit. The parameter $\Theta(k)$ is defined such that

$$\Theta(k) = \begin{cases} 0 & k = 1 \\ 1 & k > 1 \end{cases} \quad (7)$$

If k is larger than unity, in a consistent physical treatment one should take into account field-induced level shifts which are proportional to the number of photons in the field mode. Here we denote by $\beta_1^{(i)}$ and $\beta_2^{(i)}$ the intensity-dependent Stark shifts to the two levels of the i^{th} qubit, that are due to the virtual transitions to the intermediate level.

We write the Hamiltonian \hat{H} into two mutually commuting parts $\hat{H} = \hat{H}_0 + \hat{H}_{in}$, where $[\hat{H}_0, \hat{H}_{in}] = 0$,

$$\begin{aligned} \hat{H}_0 = & \omega (\hat{a}^\dagger \hat{a} + S_{ee}^{(1)} + S_{ee}^{(2)} - S_{gg}^{(1)} - S_{gg}^{(2)}), \\ \hat{H}_{in} = & \hat{a}^\dagger \hat{a} \left[\beta_1^{(1)} \hat{\sigma}_-^{(1)} \hat{\sigma}_+^{(1)} + \beta_1^{(2)} \hat{\sigma}_-^{(2)} \hat{\sigma}_+^{(2)} + \beta_2^{(1)} \hat{\sigma}_+^{(1)} \hat{\sigma}_-^{(1)} + \beta_2^{(2)} \hat{\sigma}_+^{(2)} \hat{\sigma}_-^{(2)} \right] \Theta(k) \\ & + \Delta [S_{ee}^{(1)} + S_{ee}^{(2)} - S_{gg}^{(1)} - S_{gg}^{(2)}] + \gamma_1 S_{eg}^{(1)} \hat{a}^k + \gamma_1^* S_{ge}^{(1)} \hat{a}^{\dagger k} \\ & + \gamma_2 S_{eg}^{(2)} \hat{a}^k + \gamma_2^* \hat{a}^{\dagger k} S_{ge}^{(2)}. \end{aligned} \quad (8)$$

The detuning parameter is given by $\Delta = \omega_i - k\omega$. The continuous map \mathcal{E}_t^* describing the time evolution between the qubits and the field is defined by the unitary evolution operator generated by \hat{H}_{in} such that

$$\begin{aligned} \mathcal{E}_t^* & : \mathfrak{S}_A \longrightarrow \mathfrak{S}_A \otimes \mathfrak{S}_F, \\ \mathcal{E}_t^* \rho & = \hat{U}_t (\rho^a(0) \otimes \varpi) \hat{U}_t^*. \end{aligned} \quad (9)$$

The interaction Hamiltonian, in this case, leads to an exactly solvable time evolution operator. Resuming our analysis, the time evolution operator can be written as

$$\widehat{U}_t \equiv \exp \left(-\frac{i}{\hbar} \int_0^t \widehat{H}(t') dt' \right). \quad (10)$$

A solution of equation (9) can be written as

$$\mathcal{E}_t^* \rho = \sum_{i=1}^4 \sum_{z=1}^4 \sum_{n=0}^m \sum_{l=0}^m \Omega_{iz}(n, v, t) |\Psi_i\rangle \langle \Psi_z|, \quad (11)$$

where

$$\begin{aligned} \Omega_{iz}(n, v, t) &= \sum_{l,j,s,p=1}^4 \mathfrak{R}_i^l(n) \mathfrak{R}_j^{*l}(n) \mathfrak{R}_z^{*s}(v) \mathfrak{R}_p^s(v) \Omega_{iz}(n, v, 0) e^{-it\{\lambda_l - \lambda_s\}}, \quad (12) \\ |\Psi_1\rangle &= |e_1, e_2, n - k\rangle, \quad |\Psi_2\rangle = |g_1, e_2, n\rangle, \quad |\Psi_3\rangle = |e_1, g_2, n\rangle, \\ |\Psi_4\rangle &= |g_1, g_2, n + k\rangle. \end{aligned}$$

We denote by λ_m the eigenvalues of the Hamiltonian \widehat{H}_{in} and $\mathfrak{R}_i^l(n)$ is the i^{th} element of the l^{th} eigenvector. The coefficients $\Omega_{iz}(n, v, 0)$ specify the initial conditions for the field and atomic states. The eigenvalues λ_l are to be found from a fourth-order scalar equation, the roots of which may be easily written in closed form for two identical atoms, arbitrary detuning in the absence of the Stark shifts or for two nonidentical qubits at exact resonance. For a general multiphoton interaction in the presence of Stark shifts and detuning parameter, this problem can be treated numerically. If we consider the dispersive approximation in which $\Delta \gg \mu_n \gamma$, (where $\gamma = \gamma_2 \Delta$ is the dipole coupling constant) and the second qubit is weakly coupled to the field, an explicit expression for the final state $\mathcal{E}_t^* \rho$ can be easily obtained [37,38]. In that case, it is straightforward to obtain explicit expressions for $\Omega_{iz}(n, v, t)$, namely,

$$\begin{aligned} \Omega_{11} &= A_n^t A_l^{t*} b_{n-k} b_{l-k} \cos^2 \theta_1 \cos^2 \theta_2 + B_n^t B_l^{t*} b_n b_l \sin^2 \theta_1 \cos^2 \theta_2, \\ \Omega_{12} &= A_n^t B_l^{t*} b_{n-k} b_{l-k} \cos^2 \theta_1 \cos^2 \theta_2 - B_n^t A_l^t b_n b_l \sin^2 \theta_1 \cos^2 \theta_2, \\ \Omega_{22} &= A_n^{t*} A_l^t b_n b_l \sin^2 \theta_1 \cos^2 \theta_2 + B_n^t B_l^{t*} b_{n-k} b_{l-k} \cos^2 \theta_1 \cos^2 \theta_2, \\ \Omega_{33} &= A_{n+k}^t A_{l+k}^{t*} b_n b_l \cos^2 \theta_1 \sin^2 \theta_2 + B_{n+k}^t B_{l+k}^{t*} b_{n+k} b_{l+k} \sin^2 \theta_1 \sin^2 \theta_2, \\ \Omega_{34} &= -A_{n+k}^{t*} B_{l+k}^t b_n b_l \cos^2 \theta_1 \sin^2 \theta_2 - B_{n+k}^t A_{l+k}^{t*} b_{n+k} b_{l+k} \sin^2 \theta_1 \sin^2 \theta_2, \\ \Omega_{44} &= A_{n+k}^t A_{l+k}^{t*} b_{n-k} b_{l-k} \sin^2 \theta_1 \sin^2 \theta_2 + B_{n+k}^t B_{l+k}^{t*} b_n b_l \cos^2 \theta_1 \sin^2 \theta_2, \quad (13) \end{aligned}$$

where

$$\begin{aligned} A_n^t &= \frac{1}{2} \exp(-it\{g_n - \mu_n\}) \left\{ 1 + \frac{\gamma_2}{2\mu_n} + \exp(-2i\mu_n t) \left(1 - \frac{\gamma_2}{2\mu_n} \right) \right\}, \\ B_n^t &= -\frac{\gamma_1}{2\mu_n} \sqrt{\frac{n!}{(n-k)!}} \exp(-it\{g_n - \mu_n\}) \{1 - \exp(-2i\mu_n t)\}, \quad (14) \\ \mu_n &= \sqrt{(\gamma_2^2/4) + \frac{\gamma_1^2(n+k)!}{n!}}, \quad g_n = \Delta + \gamma_2 \left(n + \frac{k}{2} \right), \end{aligned}$$

$$\Omega_{ij} = \Omega_{ji}^*, \Omega_{13} = \Omega_{14} = \Omega_{23} = \Omega_{24} = 0.$$

A downside of analyzing more complex atomic system is that analytic expressions for the final state functions and, consequently, for the matrix elements are not always available. Therefore, the greatest benefit of equation (10) which represents an analytical solution of the final state of the system for this general model, is that it directly yields a method for actually calculating any property related to the system.

4. Atomic inversion and field properties

We mainly devote the present section to consider the atomic inversion from which the phenomenon of collapse and revival can be observed [18], and see how it is affected in the present model. The population inversion expressions for each qubit can be written as

$$\langle \sigma^{(i)}(t) \rangle = \frac{1}{2} Tr \{ |e_i\rangle \langle e_i| - |g_i\rangle \langle g_i| \} \rho_i(t), \quad i = 1, 2, \quad (15)$$

where $\rho_i(t)$ is the reduced atomic density matrix of the i^{th} qubit which can be obtained by tracing out the field variables i.e.,

$$\rho_i(t) = Tr_j (\mathcal{E}_i^* \rho). \quad (16)$$

In this case, the total atomic population inversion is given by

$$\langle \sigma(t) \rangle = \frac{1}{2} (\langle \sigma^{(1)}(t) \rangle + \langle \sigma^{(2)}(t) \rangle). \quad (17)$$

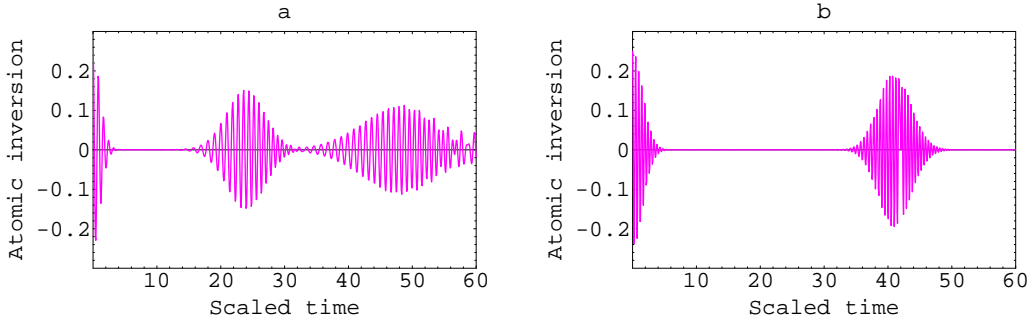


Figure 2. Time history of the total atomic inversion $\langle \sigma(t) \rangle$ as a function of the scaled time $\gamma_1 t$. Calculations assume that $k = 1, \theta_2 = \pi/4, \theta_1 = 0, m = 70, \gamma_2/\gamma_1 = 0.2$, the detuning parameter Δ has zero value, and for different values of η where (a) $\eta = 0.2$ and (b) $\eta = 0.7$.

Figure 2 is a time history of the total atomic inversion $\langle \sigma(t) \rangle$ according to equation (17) against the scaled time $\gamma_1 t$. In this figure we assume that the one-photon transition $k = 1$, the second atom starts from a maximum entangled state ($\theta_2 = \frac{\pi}{4}$) and the first atom starts from a pure state $\theta_1 = 0$, while initial field is a binomial state with $m = 70$, and for different values of the parameter η , where $\eta = 0.2$ for figure 2a and $\eta = 0.7$ for figure 2b. The detuning parameter Δ has a zero value and $\frac{\gamma_2}{\gamma_1} = 0.2$. In this case and with

a small value of η (say $\eta = 0.2$) the total atomic inversion exhibits well-known collapses and revivals. However, any change of the binomial parameter η leads to changing in the atomic inversion and consequence, increasing the parameter η , leads to elongating the revival time while the atomic inversion oscillates around the same value (see figure 2b). In general when η increases, the number of isolated revivals decreases at the same period of time. A natural next question would be: Given a quantum state of which

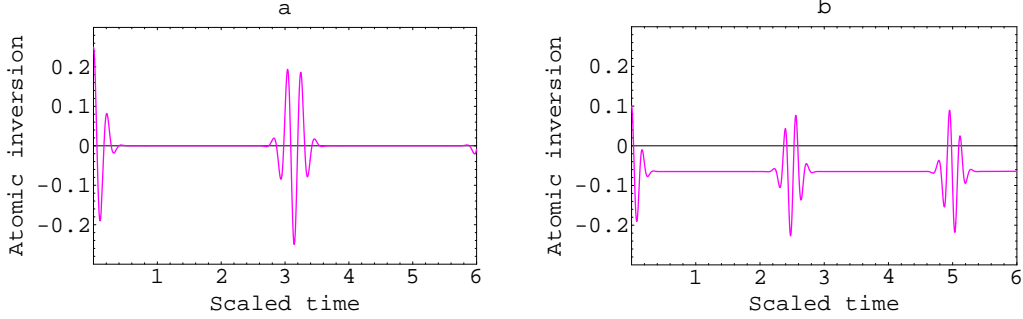


Figure 3. The evolution of the atomic inversion $\langle\sigma(t)\rangle$ as a function of the scaled time $\gamma_1 t$. Calculations assume that $k = 2$ (the two-photon processes), $\theta_2 = \pi/4, \theta_1 = 0$, $m = 70, \gamma_2/\gamma_1 = 0.2$, the detuning parameter Δ has zero value, and for different values of η where (a) $r = 1, \eta = 0.2$ and (b) $r = 0.7, \eta = 0.2$.

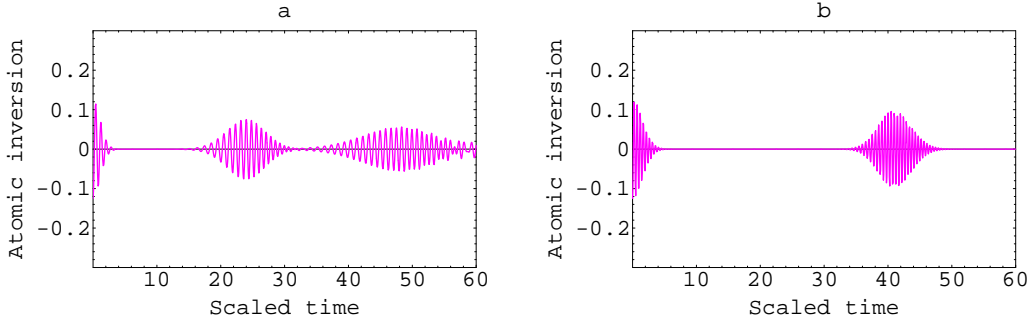


Figure 4. The evolution of the atomic inversion $\langle\sigma(t)\rangle$ as a function of the scaled time $\gamma_1 t$. Calculations assume that $k = 1, \theta_2 = \pi/4, \theta_1 = \frac{\pi}{3}$, $m = 70, \gamma_2/\gamma_1 = 0.2$, the detuning parameter Δ has zero value, and for different values of η where (a) $\eta = 0.2$ and (b) $\eta = 0.7$.

one knows that it is entangled, how can $\langle\sigma(t)\rangle$ be affected by a multiphoton transition? One may envision, for example, the situation that a two-photon process is involved (i.e. $k = 2$). In figure 3, we consider this case in which the Stark shift will be taken into account (we set $k = 2$ and the other parameters are the same as in figure 2). We see that the total atomic inversion has rapid oscillations with a periodical collapses and revivals. This discussion has clearly demonstrated that the general behavior of the total atomic inversion, when the two-photon transition is involved, is remarkably affected by changing the number of quanta and $\langle\sigma(t)\rangle$ is almost periodic. This periodicity follows a

consequence of the fact that the generalized Rabi frequency in the two-photon transition is proportional to n rather than to \sqrt{n} which is the case in the single-photon process. In the presence of the Stark shifts namely $r = \sqrt{\beta_2^{(i)}/\beta_1^{(i)}}$, we note that the Rabi frequency as well as the temporal width of the oscillations packets decrease (see figure 3b). The most obvious difference, is that the population inversion collapses to a nonzero value with the inclusion of Stark shifts but to a zero value without it. This fact highlights an important difference between the two situations.

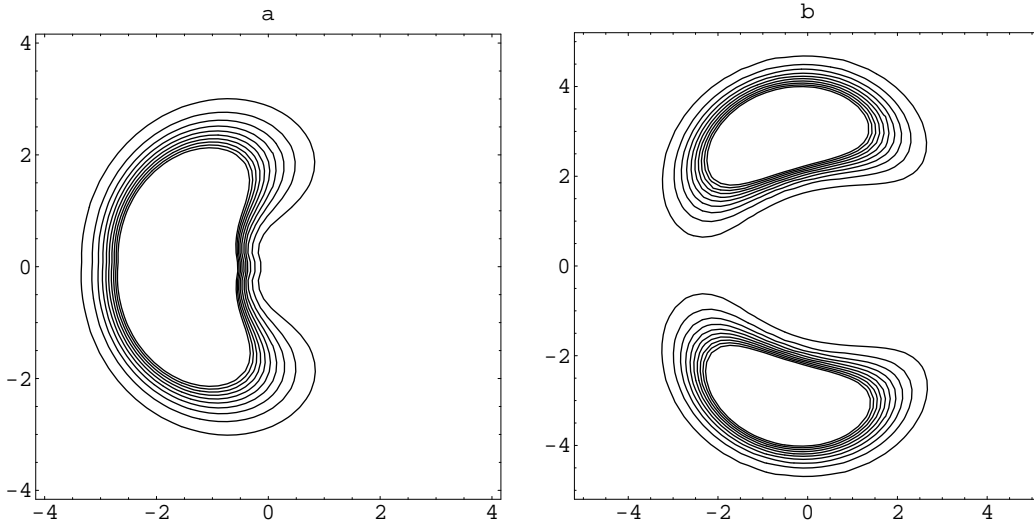


Figure 5. Contour plot of the field reduced density matrix quasiprobability distribution function against $X = Re.(\beta)$ and $Y = Im.(\beta)$. Calculations assume that $k = 1, \theta_2 = \pi/4, \theta_1 = 0, m = 70, \gamma_2/\gamma_1 = 0.2$, and the detuning parameter Δ has zero value, where (a) $\gamma_1 t = \frac{5\pi}{2}, \eta = 0.2$ and (b) $\gamma_1 t = \frac{5\pi}{2}, \eta = 0.7$.

In what follows we shall choose the parameters to show the first atom starts also from a mixed state, i.e $\theta_1 = \frac{\pi}{3}$. In this case the evolution of the atomic inversion still exhibits Rabi oscillations, showing collapses and revivals. The oscillations are independent of θ_1 , but θ_1 strikingly affects the amplitude of the inversion (see figure 4). As soon as we take θ_1 effect into consideration it is easy to realize that the amplitude of the oscillations is decreased. Furthermore if we take larger values of the binomial parameter η , the revival time is elongated and the atomic inversion oscillates around zero.

At this end and after discussing a particular aspect of the atomic inversion in the multi-photon two two-level qubits model with the initial field prepared in the binomial state, which clearly exhibits the collapses-revivals phenomenon and provide us with information about the discrete nature of the quantum qubit-cavity field eigenvalues, we are going to focus our attention on the representation of the field in phase space which provides some aspects of the field dynamics. Perhaps the most convenient quasiprobability to be used in this kind of problem is the Q -function. The first step to be taken is the calculation of the reduced density operator for the field $\rho_F(t)$, and

then we get the Q -function as

$$Q(x, y, t) = \frac{1}{\pi} \langle \zeta | \rho_F(t) | \zeta \rangle, \quad (18)$$

where $|\zeta\rangle$ is a coherent state with amplitude $\zeta = x + iy$. The Q -function is not only a convenient tool to calculate expectation values of anti-normally ordered products of operators, but also gives us a new insight into the mechanism of interaction in the model under consideration. Figure 5 shows a contour plot of the reduced density matrix Q -function quasiprobability for different values of the binomial parameter η . When η increases, the Q -function bifurcates into two blobs rotating in the complex coherent state parameter plane in the clockwise and counterclockwise directions with the same speed. The collision of the blobs corresponds to the revival. This can be clearly seen if we compare the numerical calculations for inversion and Q -function.

5. Concurrence

The characterization and classification of entanglement in quantum mechanics is one of the cornerstones of the emerging field of quantum information theory. Although an entangled two-qubit state $\mathcal{E}_t^* \rho$ is not equal to the product $\mathcal{E}_t^* \rho_1$ and $\mathcal{E}_t^* \rho_2$ of the two single-qubit states contained in it, it may very well be a convex sum of such products. In general it is known that microscopic entangled states are found that to be very stable, for example electron-sharing in atomic bonding and two-qubit entangled photon states generated by parametric down conversion. Entanglement as one of the most nonclassical features of quantum mechanics is usually arisen from quantum correlations between separated subsystems which can not be created by local actions on each subsystem.

As more and more experimental realizations of entanglement sources become available, it is necessary to develop different methods of measuring the entanglement produced by different sources [39]. An ensemble is specified by a set of pairs $\{(p_i, |\psi_i\rangle)\}_{i=1}^N$, consisting of N state vectors $|\psi_i\rangle$ and associated statistical weights p_i , and, N is called the cardinality of the ensemble. The concurrence of a bipartite state (i.e., a state over the bi-partite Hilbert space $\mathfrak{S}_A \otimes \mathfrak{S}_F$) is defined by an almost magic formula [30,31]

$$C_{\mathcal{E}_t^* \rho}(t) = \max \{0, \lambda_1 - \lambda_2 - \lambda_3 - \lambda_4\}. \quad (19)$$

We denote by λ_i the square roots of the eigenvalues of $(\mathcal{E}_t^* \rho) \times \widetilde{(\mathcal{E}_t^* \rho)}$ in descending order, where

$$\widetilde{(\mathcal{E}_t^* \rho)} = (\sigma_{y_1} \otimes \sigma_{y_2}) (\mathcal{E}_t^* \rho)^* (\sigma_{y_1} \otimes \sigma_{y_2}). \quad (20)$$

where σ_{y_i} is the Pauli matrix. The importance of this measure follows from the direct connection between concurrence and entanglement of formation. It has been shown that [30] the entanglement of formation of an arbitrary state $\mathcal{E}_t^* \rho$ is related to the concurrence $C_{\mathcal{E}_t^* \rho}(t)$ by a function

$$E_F(C_{\mathcal{E}_t^* \rho}(t)) = \pi^+(t) \log \pi^+(t) + \pi^-(t) \log \pi^-(t), \quad (21)$$

where

$$\pi^\pm(t) = \frac{1}{2} \left(1 + \sqrt{1 - C_{\mathcal{E}_t^* \rho}^2(t)} \right). \quad (22)$$

The entanglement of formation is monotonically increasing with respect to the increasing concurrence. If we could write the general bipartite pure state as [40,31]

$$|\psi(t)\rangle \equiv \sum_{i,j=0}^{d-1} \sum_{n=0}^{\infty} \wp_{ij}(n,t) |i,j,n\rangle, \quad (23)$$

in this case, the concurrence can be calculated as

$$\begin{aligned} C_{\mathcal{E}_t^* \rho}(t) &= \left\{ 2 \left[1 - \text{Tr}(\rho_A^2(t)) \right] \right\}^{\frac{1}{2}} \\ &= \left\{ \sum_{n=0}^{\infty} \sum_{i,j,l,k=0}^d |\wp_{ik}(n,t)\wp_{jm}(n,t) - \wp_{im}(n,t)\wp_{jk}(n,t)|^2 \right\}^{\frac{1}{2}}. \quad (24) \end{aligned}$$

The concurrence $C_{\mathcal{E}_t^* \rho}(t)$ as a measure of the degree of entanglement ensures the scale between 0 and 1 and monotonously increases as entanglement grows. A note of caution about how to interpret the state of a physical system in terms of quantum entanglement may be in place here. The previous standard definitions of quantum entanglement tacitly assume that, every state in the bipartite or multipartite Hilbert space is in principle available as a physical state and local as well as global quantum operations, measurements and unitary transformations, can be performed on the Hilbert space.

5.1. Results

We now discuss applications of the above equation to specific situations. As stated above, an important situation is that, when $C_{\mathcal{E}_t^* \rho}(t) = 0$ the two qubits are separable and $C_{\mathcal{E}_t^* \rho}(t) = 1$ indicates maximum entanglement between the two qubits. In our numerical examples we have used physical parameters from some recent experiments [22, 41], but extrapolated the qubit transit time t to rather large values of $\gamma_1 t$. It is, of course, an experimental challenge to obtain a one-qubit source and atomic lifetimes of the atomic states involved such that these large values of $\gamma_1 t$ can be reached. An interesting question is whether or not the entanglement is affected by the different parameters of the present system with the initial state in which one of the qubits is prepared in its excited state and the other in the mixed state. In particular, the mixed state parameter θ_2 , the scaled time $\gamma_1 t$, and the parameters from the initial state of the field (m, η) . A numeric evaluation of the concurrence as an entanglement measure leads to the plot in figures 6-10. We now pause to touch on certain concurrence features when $\eta \approx 0$ (i.e., the coherent state), the mean photon number $\eta m = 20$ for figure 6a and $\eta m = 10$ for figure 6b. The maximum value of the entanglement increased as the mean photon number is decreased (see figure 6), but the entanglement vanishes as the time goes on for large values of the mean photon number this is not the case when \bar{n} takes small values (see figure 6b). It is interesting to note that, the maximum entanglement is achieved when $\theta_2 = \frac{n\pi}{4}$, $n = \pm 1, \pm 3, \pm 5, \dots$ while $C_{\mathcal{E}_t^* \rho}(t) \approx 0$, for

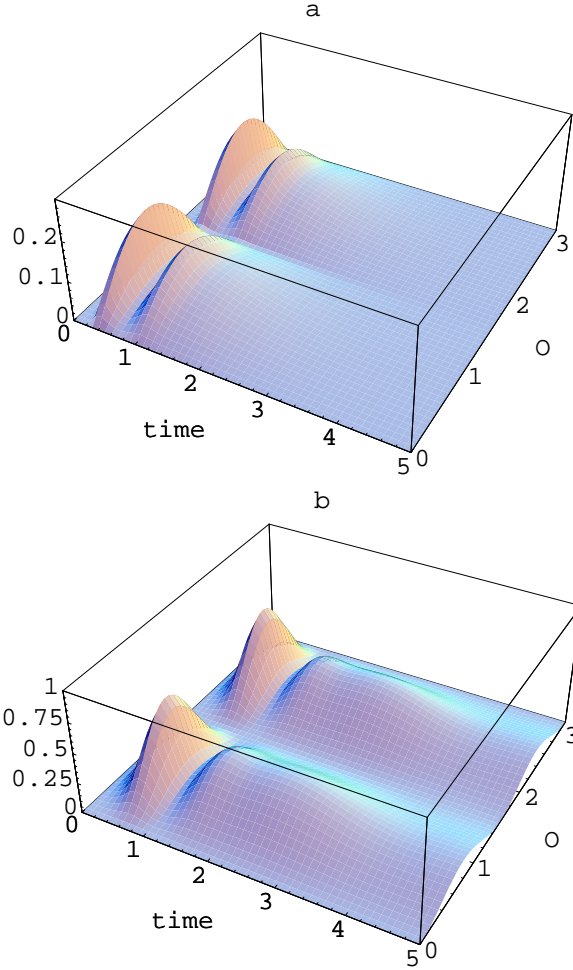


Figure 6. Plot of the concurrence $C_{\mathcal{E}_t^* \rho}(t)$ as a function of the scaled time $\gamma_1 t$ and θ_2 . The field initially in the binomial states with $\eta = 0$, $k = 1$, $\Delta = 0$, $\gamma_2/\gamma_1 = 0.2$, and for different values of the mean photon number $\eta m = \bar{n}$, where (a) $\bar{n} = 20$ and (b) $\bar{n} = 8$.

$\theta_2 = \frac{m\pi}{2}$, $m = 0, \pm 1, \pm 2, \dots$. Also, the entanglement shows symmetry around $\theta_2 = 0$. Put differently, with different values of η , such as $\eta=0.7$, one will have a very small amount of entanglement at the initial period of time only and this amount disappear when the time goes on (see figure 7a). Indeed, the comparison of plots figure 6a and figure 7a where $\eta = 0$ and $\eta = 0.7$, respectively demonstrates that the entanglement in both cases has somewhat similar behavior corresponding to different values of θ_2 . In accord with the initial conditions $\eta = 0.7$ and $m = 70$, figure 7b shows more oscillations at the same period of time while the entanglement survive in this case longer. Also, small amount of entanglement is repeated several times with the time development. At the period $2 \leq \gamma_1 t \leq 3$, the entanglement shows small oscillations throughout the manipulations as a result of increasing the binomial parameter $\eta = 0.9$. The comparison between figure 7a and figure 7b shows the obvious effects of the binomial parameter η in the dynamics of the system. Next, we will analyze the influence of dispersive approximation

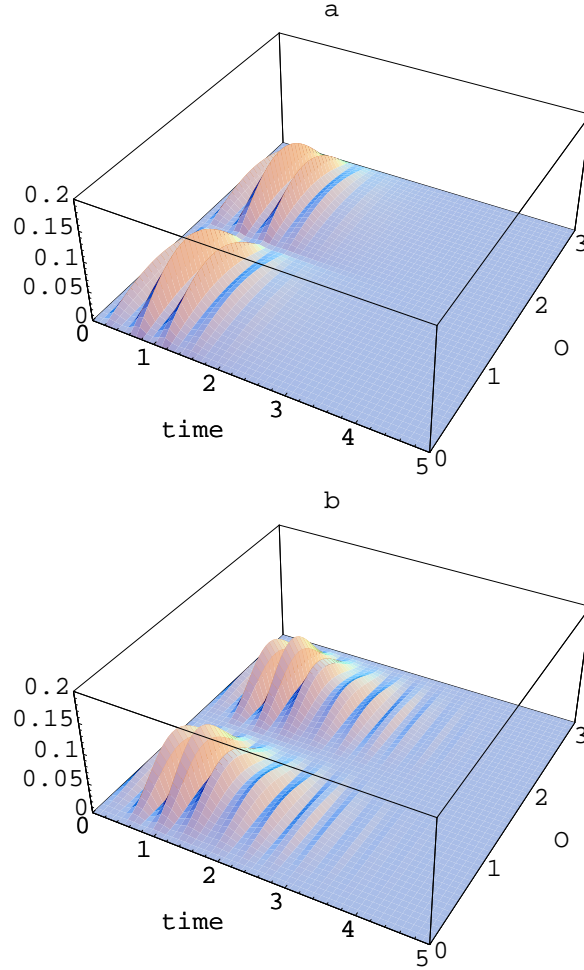


Figure 7. Plot of the concurrence $C_{E_{t\rho}}(t)$ as a function of the scaled time $\gamma_1 t$ and θ_2 . The field initially in the binomial states with $\bar{n} = 20$, $k = 1$, $\Delta = 0$, $m = 70\gamma_2/\gamma_1 = 0.2$, and for different values of η where (a) $\eta = 0.7$ and (b) $\eta = 0.9$.

on the appearance or disappearance phenomenon of the entanglement previously found. Dispersive effects can be conveniently incorporated by assuming that $\gamma_2 \ll \gamma_1$, (such as $\frac{\gamma_2}{\gamma_1} = 0.01$). It is remarkable to see that with $\eta = 0.7$, entanglement is nearly washed out for the initial stage of the interaction time. While more oscillations have been observed when the time goes on (see figure 8a). The situation is changed for $\eta = 0.9$ (see figure 8b), in this case the maximum entanglement increased further and start earlier. The initial period in which the entanglement washed out in figure 8a decreased with increasing the parameter η . Also, the maximum value of the entanglement is increased with increasing η . The number of quanta effect on the entanglement is particularly pronounced as this number takes large values. In figure 9a the entanglement is plotted as a function of $\gamma_1 t$ and θ_2 for $k = 2$. However, we note from this plot that the maximum amount of the two-qubit entanglement indeed does move closer to the point at $\gamma_1 t = 0$. Again we notice some similarities with other plots in the sense that there is

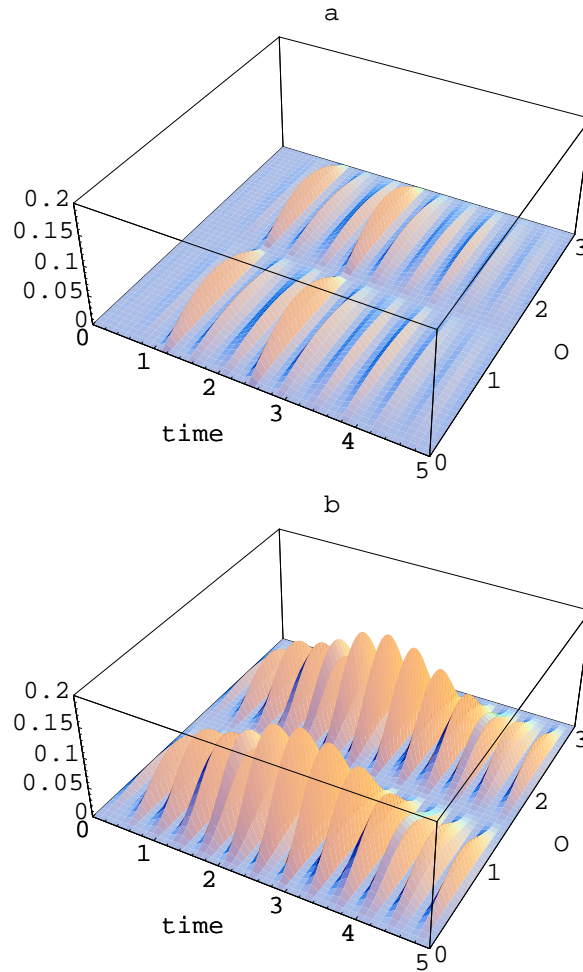


Figure 8. The same as figure 2 but $\gamma_2/\gamma_1 = 0.01$.

no entanglement for $\theta_2 = \frac{m\pi}{2}$ and maximum value at $\theta_2 = \frac{n\pi}{4}$, (see figure 9a). From our further calculations (which were not presented here) it is clear that we can get the same amount of entanglement using the present measure (concurrence) and the negativity as a measure of entanglement, in agreement with our previous result [42]. Also, the qubits and radiation subsystems exhibit alternating sets of collapses and revivals due to the initial mixed states of the qubits and radiation employed here. Let us now consider the situation when the qubits are initially both in mixed state and nonzero detuning. It is surprising that a nonresonant case (nonzero detuning) can entangle two qubits depending on their atomic initial preparation. First of all, we note that the entanglement appears only for the initial period of the interaction time. These properties show that the role played by the detuning on the entanglement is essential.

The above results pose two intriguing questions: (i) Why does the entanglement become maximum for $\theta_2 = \frac{n\pi}{4}$, and takes zero value for $\theta_2 = 0, \frac{n\pi}{2}$?, (ii) Why does the entanglement due to the concurrence behave essentially in a similar way with different values of the mixed state parameter whatever values of the other parameters? In what

follows, we propose an analytic expressions which can give an answer to these questions. We now first analyze the reason why the concurrence does not exceed zero value when $\theta_2 = 0$. To prove that analytically, one may first consider $\theta_i = 0$, then we have only nonzero values of Ω_{11}, Ω_{12} and Ω_{22} and all the other Ω_{ij} vanish, i.e. the coefficients Ω_{ij} in equation (13) reduce to

$$\begin{aligned}\Omega_{11} &= A_n^t A_l^{t*} b_{n-k} b_{l-k}, \\ \Omega_{12} &= A_n^t B_l^{t*} b_{n-k} b_{l-k}, \\ \Omega_{22} &= B_n^t B_l^{t*} b_{n-k} b_{l-k}.\end{aligned}\tag{25}$$

Using these coefficients with the above definition of the concurrence we easily find that $C_{\mathcal{E}_t^* \rho}(t) = 0$, this is also in agreement with the numerical calculations. On the other hand, if we consider the first qubit in its excited state and the second qubit in a mixed state, then equation (13) reduces to,

$$\begin{aligned}\Omega_{11} &= A_n^t A_l^{t*} b_{n-k} b_{l-k} \cos^2 \theta, \\ \Omega_{12} &= A_n^t A_l^{t*} b_{n-k} b_{l-k} \cos^2 \theta, \\ \Omega_{22} &= B_n^t B_l^{t*} b_{n-k} b_{l-k} \cos^2 \theta, \\ \Omega_{33} &= A_{n+k}^t A_{l+k}^{t*} b_n b_l \sin^2 \theta, \\ \Omega_{34} &= -A_{n+k}^t B_{l+k}^{t*} b_n b_l \sin^2 \theta, \\ \Omega_{44} &= B_{n+k}^t B_{l+k}^{t*} b_n b_l \sin^2 \theta.\end{aligned}\tag{26}$$

For simplicity we used θ instead of θ_2 . In this case the concurrence is given by

$$C_{\mathcal{E}_t^* \rho}(t) = \left| \frac{\sin 2\theta}{2} \right| \left\{ \sum_{n=0}^{\infty} b_n^2 b_{n-k}^2 \left| A_n^t B_{n+k}^{t*} - B_n^t A_{n+k}^{t*} \right|^2 \right\}^{\frac{1}{2}}.\tag{27}$$

From equation (27) we see that for $\theta = \frac{n\pi}{4}$, we will get maximum value of $C_{\mathcal{E}_t^* \rho}(t)$ and for $\theta = \frac{n\pi}{2}$, $C_{\mathcal{E}_t^* \rho}(t) = 0$. It is also clearly from this equation, the concurrence depend on the amplitude of the initial binomial state. Here, we clarify that it can be done by using the different initial state, which is strongly affected by the atomic number representation. This naturally leads to the use of occupation numbers of different single-qubit basis states in quantifying multi-qubit entanglement even when the number of qubits is conserved. The occupation-numbers of different modes have already been used in quantum computing [43]. It is important to refer here to the work in Ref. [44] in which experimentally a superposition state of the ground state and a non-maximally entangled antisymmetric state in two trapped ions has been realized. In the experiment two trapped barium ions were sideband cooled to their motional ground states. Transitions between the states of the ions were induced by Raman pulses using co-propagating lasers. The non-maximally entangled state was used [45] to demonstrate the intrinsic difference between quantum and classical information transfers. The difference arises from the different ways in which the probabilities occur and is particularly clear in terms of entangled states.

Before we conclude, it is necessary to give a brief discussion on the experimental realization of the present model. It was reported that the cavity can have a photon

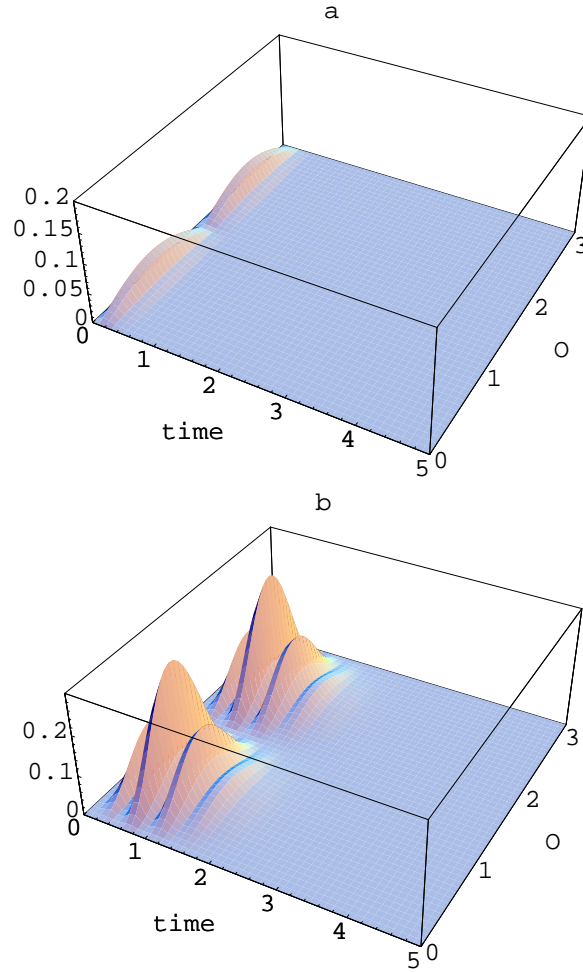


Figure 9. Plot of the concurrence $C_{E_t^* \rho}(t)$ as a function of the scaled time $\gamma_1 t$ and θ_2 . The field initially in the binomial states with $\bar{n} = 20$, $m = 70$, $\eta = 0.7$, $\gamma_2/\gamma_1 = 0.2$, where (a) $k = 2$, $\Delta = 0$ and (b) $k = 1$, $\frac{\Delta}{\gamma_1} = 10$.

storage time of $T = 1$ ms (corresponding to $Q = 3 \times 10^8$). The radiative time of the Rydberg atoms with the principle quantum numbers 49, 50 and 51 is about 2×10^{-4} s. The coupling constant of the atoms to the cavity field is $2\pi \times 24$ kHz [46]. The experiment may be described schematically as follows: a stream of pairs of rubidium atoms in circular Rydberg states, time and velocity selected, was sent through a resonant cavity [47]. Each pair consisted of one atom in a state with principle quantum number 51, and the other in a state with principle quantum number 50, the frequency of transition between the two states being 51.1 GHz. Also, there was an experiment [47] in which the phase of oscillation of each of two entangled qubits is individually controlled and can be adjusted to provide the necessary values for testing a Bell inequality.

6. Conclusion

To sum up, in the main part of this paper we have investigated the properties of the dynamically emerging entanglement in the multiphoton two two-level qubits. We have treated the more general case where initial states of the two qubits can be mixed with a binomial state of the field. We have obtained an exact solution of the density operator taking into account the dispersive limit, and thus provides insight into the behavior of more complicated two-qubit systems. We have investigated the interaction of the binomial states (which reduce to number and coherent states in two different limits) with atomic systems in the framework of the two two-level qubits, and describe the response of the atomic system as it varies between the Rabi oscillations and the collapse-revival mode and investigate the total atomic inversion and the quasiprobability distributions. The idea of using the concurrence as an entanglement measure offers many attractive features. Entanglement is measured via the concurrence, currently used only for an arbitrary system of two qubits, but similar analysis can in principle be applied to other systems such as a bipartite system with arbitrary dimensions. As we anticipated, this system exhibits some novel features in comparison with the single qubit system. We have found that some different regimes occur, depending on the actual initial joint product state, the number of quanta and the binomial state parameters. It was demonstrated that quantum entanglement is stored in the model system considered, and that the nature of this entanglement is strongly dependent on the detuning of the atomic levels, an effect that may have important consequences in other nonlinear processes.

- [1] Messikh A, Ficek Z and Wahiddin M R B 2003 *J. Opt. B: Quantum Semiclass. Opt.* **5** L1;
Zhou L, Song H S and Li C 2002 *J. Opt. B: Quantum Semiclass. Opt.* **4** 425;
Bennett C H, Brassard G, Crepeau C, Jozsa R, Peres A, and Wootters W K 1993 *Phys. Rev. Lett.* **70** 1895.
- [2] Bouwmeester D, Pan J-W, Mattle K, Eibl M, Weinfurter H, and Zeilinger A, *Nature* **390** 575;
Kim M S, Jinhyoung Lee, Ahn D and Knight P L 2002 *Phys. Rev. A* **65** 040101.
- [3] Deutsch D and Jozsa R 1992 *Proc. R. Soc. Lond. A* **439** 553.
- [4] Abdel-Aty M 2000 *J. Phys. B: At. Mol. Opt. Phys.* **33** 2665;
Abdel-Aty M, and Obada A-S F 2003 *Eur. Phys. J. D* **23** 155;
Simon D R 1997 *SIAM J. Comput.* **26** 1474.
- [5] Grover L K 1997 *Phys. Rev. Lett.* **79** 325;
Senitzky I R 2002 *J. Phys. B: At. Mol. Opt. Phys.* **35** 3029.
- [6] Rudolph O 2001 *J. Math. Phys.* **42** 5306;
Williams C P and Clearwater S H 1998 *Explorations in Quantum Computing* (New York: Telos, Springer-Verlag).
- [7] Abdel-Aty M 2003 *J. Math. Phys.* **44** 1457 and *Virtual J. Quant. Infor.* April 2003, Volume 3, Issue 4.
- [8] Sorensen A and Molmer K 2000 *Phys. Rev. A* **62** 022311.
- [9] Horodecki M, *Phy. Rev. A*, **57** 3364 (1998).
- [10] Bennett C H 1995 *Phys. Today* **48** 24.
- [11] Terhal M, Horodecki M, Leung D W, DiVincenzo D P 2002 *J. Math. Phys.* **43** 4286.
- [12] Rudolph O 2001 *J. Math. Phys.* **42** 5306.
- [13] Barenco A, Bennett C H, Cleve R, DiVincenzo D P, Margolus N , Shor P, Sleator T, Smolin J A and Weinfurter H 1995 *Phys. Rev. A* **52** 3457.
- [14] Iwai T and Hirose T 2002 *J. Math. Phys.* **43** 2907.

- [15] Ficek Z and Tanas R 2002 Phys. Rep. **372** 369.
- [16] Agarwal G S 1974, Quantum Optics, Springer Tracts in Modern Physics Vol. 70 (Springer-Verlag, Berlin).
- [17] Milman P, and Mosseri R arXiv: quant-ph/0302202;
Verstraete F and Verschelde H 2002 Phys. Rev. A **66** 022307.
- [18] Kudryavtsev I K, Lambrecht A, Moya-Cessa H and Knight P L 1993 J. Mod. Opt. **40** 1605;
Obada A-S F and Omar Z M 1993 J. Egypt. Math. Soc. **1** 63.
- [19] Jex I 1990 Quantum Optics **2** 433; 1990 J. Mod. Opt. **39** 835.
- [20] Song T Q, Feng J, Wang W Z and Xu J Z 1995 Phys. Rev. A **51** 2648.
- [21] Kudryavtsev I K and Knight P L 1993 J. Mod. Opt. **40** 1673.
- [22] Titttonen I, Stenhplm S and Jex I 1996 Opt. Commun. **124** 271.
- [23] Abdel-Aty M 2003 J. Opt. B: Quantum Semiclass. Opt. **5** 349.
- [24] Ashraf M M 1999 Opt. Commun. **166** 49.
- [25] Ashraf I and Toor A H 2000 J. Opt. B: Quantum Semiclass. Opt. **2** 772;
- [26] Ashraf M M 2001 J. Opt. B: Quantum Semiclass. Opt. **3** 39.
- [27] Yu Shi 2003 Phys. Rev. A **67** 024301.
- [28] Tessier T E, Deutsch I H, Delgado A and Fuentes-Guridi I 2003 arXiv:quant-ph/0306015.
- [29] Kim M S, Lee J, Ahn D and Knight P L 2002 Phys. Rev. A **65** 040101.
- [30] Wootters W K 1998 Phys. Rev. Lett. **80**, 2245.
- [31] Hill S and Wootters W K 1997 Phys. Rev. Lett. **78** 5022;
Hughston L, Jozsa R and Wootters W 1993 Phys. Lett. A **183** 14;
Lozinski A, Buchleitner A, Zyczkowski K and Wellens T 2003 Europhys. Lett. **62** 168;
Rungta P, Bužek V, Caves C M, Hillery M and Milburn G J. 2001 Phys. Rev. A **64** 042315.
- [32] Fan H, Matsumoto K and Imai H 2003 J. Phys. A: Math. Gen. **36** 4151.
- [33] Stoler D and Saleh B E A and Teich M C 1985 Opt. Acta **32** 345.
- [34] Mahran M H, Abdalla M S, Obada A-S F and El-Orany F A A 1998 Nonlinear Opt. **19** 189.
- [35] Vidal G and Tarrach R 1999 Phys. Rev. A **59** 141.
- [36] Shor P W 2002 J. Math. Phys. **43** 4334.
- [37] Brune M, Haroche S, Raimond J M, Davidovich L and Zagury N 1992 Phys. Rev. A **45** 5193.
- [38] Roversi J A, Vidiella-Barranco A and Moya-Cessa H 2003 Mod. Phys. Lett. B **17** 219.
- [39] Mair A, Vaziri A, Weihs G, and Zeilinger A 2001 Nature **412** 313.
- [40] Albererio S and Fei S M 2001 J. Opt. B: Quant. Semiclass. Opt. **3** 223.
- [41] Benson O, Raithel G and Walther H 1994 Phys. Rev. Lett. **72** 3506 and Dynamics of the
Micromaser Field in Electron Theory and Quantum Electrodynamics: 100 Years Later, Ed.
Dowling J P 1997 (Plenum Press, New York).
- [42] Obada A-S F and Abdel-Aty M 2003 J. Math. Phys. preprint.
- [43] E Knill, R Laflamme and Milburn G J 2001 Nature (London) **409** 46.
- [44] Turchette Q A, Wood C S, King B E, Myatt C J, Leibfried D, Itano W M, Monroe C and Wineland
D J 1998 Phys. Rev. Lett. **81** 3631.
- [45] Franke S, Huyet G, and Barnett S M 2000 J. Mod. Opt. **47** 145.
- [46] Brune M, E Hagley, Dreyer J, Maitre X, Maali A, Wunderlich C, Raimond J M, and Haroche S
1996 Phys. Rev. Lett. **77** 4887.
- [47] Hagley E, Maitre X, Nogues G, Wunderlich C, Brune M, Raimond J M and Haroche S 1997 Phys.
Rev. Lett. **79** 1.
- [48] Rowe M A, Kielpinski D, Meyer V, Sackett C A, Itano W M, Monroe C, and Wineland D J 2001
Nature **409** 791.